

Figure 6 Simulated and measured frequency responses of the bandpass filter

cated bandpass filter is at 2.47 GHz and the fractional bandwidth is 5%. The measured insertion loss and return loss of the filter is -3.68 and -14.92 dB, respectively. The measured center frequency, insertion loss and return loss of the fabricated filter are in agreement with simulated results.

ACKNOWLEDGMENT

The authors are grateful to the National Science Council of R.O.C. for financial support under the project No. NSC 94-2215-E-214-007.

REFERENCES

1. M.L. Hsieh, L.S. Chen, S.M. Wang, C.H. Sun, M.H. Weng, M.P. Houg, and S.L. Fu, Low-temperature sintering of microwave dielectrics (Zn,Mg)TiO₃, *Jpn J Appl Phys* 44 (2005), 5045-5048.
2. R. Levy, R.V. Snyder, and G. Matthaei, Design of microwave filters, *IEEE Trans Microwave Theory Tech* 50 (2002), 783-793.
3. J.S. Hong and M.J. Lancaster, Couplings of microstrip square open-loop resonators for cross-coupled planar microwave filters, *IEEE Trans Microwave Theory Tech* 44 (1996), 2099-2109.
4. J.T. Kuo, M.J. Maa, and P.H. Lu, A microstrip elliptic function filter with compact miniaturized hairpin resonators, *IEEE Microwave Guided Wave Lett* 10 (2000), 94-95.
5. C.S. Ahn, J. Lee, and Y.S. Kim, Design flexibility of an open-loop resonator filter using similarity transformation of coupling matrix, *IEEE Microwave Wireless Compon Lett* 15 (2005), 262-264.
6. J.S. Hong and M.J. Lancaster, Design of highly selective microstrip bandpass filters with a single pair of attenuation poles at finite frequencies, *IEEE Trans Microwave Theory Tech* 48 (2000), 1098-1107.
7. J.S. Hong and M.J. Lancaster, *Microstrip filters for RF/microwave applications*, Wiley, New York, 2001, p. 318.
8. Zeland Software, IE3D 6.0, New York, 1999.

© 2007 Wiley Periodicals, Inc.

RAPID PROTOTYPING OF CERAMIC MILLIMETERWAVE METAMATERIALS: SIMULATIONS AND EXPERIMENTS

Yoonjae Lee,¹ Xuesong Lu,² Yang Hao,¹ Shoufeng Yang,² Rich Ubic,² Julian R. G. Evans,² and Clive G. Parini¹

¹ Department of Electronic Engineering, Queen Mary, University of London, Mile End Road, London E1 4NS, United Kingdom

² Department of Materials, Queen Mary, University of London, Mile End Road, London E1 4NS, United Kingdom

Received 29 January 2007

ABSTRACT: Rapid prototyping by an extrusion freeforming technique, of ceramic metamaterials based on a woodpile structure at millimeter-wave frequencies has been performed. The finite difference time domain technique is applied for the design and characterization of the proposed metamaterials. The transmittance of the millimeterwave metamaterials is measured in the range of 75–110 GHz. Both measurement and simulation results are in good agreement. © 2007 Wiley Periodicals, Inc. *Microwave Opt Technol Lett* 49: 2090–2093, 2007; Published online in Wiley InterScience (www.interscience.wiley.com). DOI 10.1002/mop.22697

Key words: millimeterwave; EBG; metamaterial; woodpile; freeforming fabrication

1. INTRODUCTION

Millimeterwave systems are becoming increasingly important in many scientific, civil, and military applications because they can provide wider bandwidth for transmitting large amount of data and better resolution in radar systems. In recent years, it has been demonstrated by various groups that novel devices can be realized using electromagnetic bandgap (EBG) structures, a class of metamaterials. EBG structures, also known as photonic bandgap structures (PBG) [1, 2] in optics, are now finding numerous applications at microwave and millimeterwave frequencies [3, 4]. In general, EBG structures consist of periodic dielectric or metallic elements, and exhibit forbidden frequency bands (bandgap). The full potential of EBG structures can be utilized with a full three-dimensional (3D) bandgap. Thus, rapid and cost-effective fabrication techniques for 3D EBG structures are of significant importance. The woodpile structure shown in Figure 1, also called a layer-by-layer structure, consists of stacked diffraction gratings, in which adjacent layers are perpendicular to each other. This structure possesses face-centered-tetragonal symmetries and provides a full 3D bandgap. Such a periodic structure can be easily fabricated for microwave applications using columns of individually machined dielectric materials with preferable dimensions. However, at millimeterwave frequencies, conventional machining would not be convenient because of small dimensions (50–500 μm). Various sophisticated microfabrication techniques such as silicon lithography and wafer fusion are available for microstructures, but those are more appropriate for terahertz and photonic wavelength applications, and would be costly to fabricate 3D structures with large number of layers for applications at W-band (75–110 GHz). The team at University of Michigan [5] has used indirect solid freeforming to make alumina woodpile structures by casting ceramic slurry into a solid freeformed mould. In this letter, we present a direct rapid prototyping method for constructing 3D EBG materials for millimeterwave applications, with a possible extension to higher frequencies based on extrusion freeforming of ceramic materials [6]. The proposed fabrication method can also be versatile for constructing curved geometries and creating defects in layered structures.

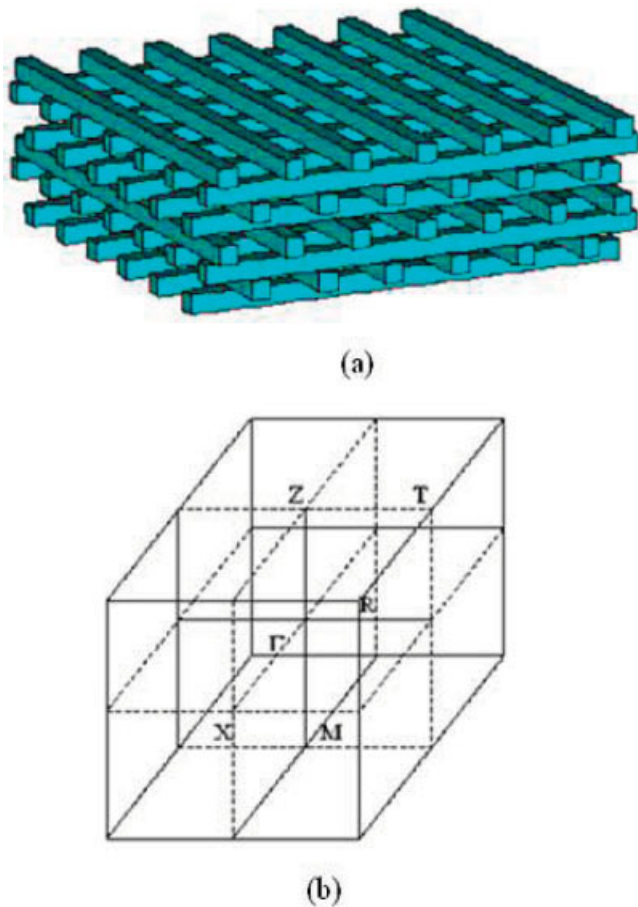


Figure 1 (a) Geometry of the woodpile structure, (b) Brillouin zone defined for the unit cell. [Color figure can be viewed in the online issue, which is available at www.interscience.wiley.com]

2. WOODPILE EBG DESIGN

We choose to design EBG structures for around 95 GHz, at which frequency security imaging radars widely operate. We first determine the rod width (w) and period (a) based on the bandgap frequency found in the dispersion diagram. We use the finite difference time domain (FDTD) method for the computation of the dispersion diagram of the woodpile EBG structure [7, 8]. Other methods are also available [9, 10]. A nominal permittivity value of alumina material ($\epsilon_r = 9.6$) at 95 GHz [11] was used throughout the simulation. Figure 2 shows the computed dispersion diagram of the woodpile structure with $w/a = 0.25$, where w is the width of the dielectric rod, and a is the period of the square lattice. A complete bandgap exists between the normalized frequencies of 0.45 and 0.51. The design parameters for the woodpile have been found as $w = 0.4$ mm and $a = 1.6$ mm with $\epsilon_r = 9.6$. To verify the existence of the bandgap, the transmission property was characterized along the vertical direction (Γ -Z direction) with horizontally polarized electric field. Figure 3 shows the simulated transmittance of the designed woodpile EBG structure with 1–3 periods in vertical direction. In the vertical direction, bandgap exists between the normalized frequencies of 0.45 and 0.63, which correspond to 84 and 118 GHz in actual frequency. The attenuation of the electric field within the bandgap is clear, while at the frequencies outside the bandgap, the wave is propagating with very little attenuation.

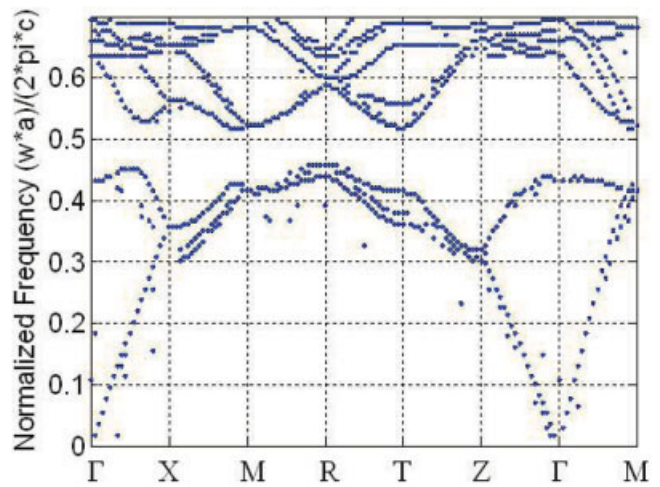


Figure 2 Computed dispersion diagram. [Color figure can be viewed in the online issue, which is available at www.interscience.wiley.com]

3. FABRICATION OF MILLIMETERWAVE EBG STRUCTURE

The designed woodpile structure has been fabricated using the extrusion freeforming technique. The fabrication facility at Queen Mary, University of London (QMUL) is currently capable of making ceramic filament as thin as 80 μm with 20 μm spacing. The high purity alumina powder (99.992%, $d_{50} = 0.48$ μm , ex Condea Vista, Tucson, Arizona) was used as a dielectric material. The poly vinyl butyral (PVB), grade BN18 (Whacker Chemicals, UK) was used as the binder with addition of a grade of poly ethylene glycol (PEG) that is liquid at ambient temperature, (MWt = 600, VWR, UK). Mixtures of 75 wt% PVB and 25 wt% PEG600 were fully dissolved in propan-2-ol (GPR, VWR, UK). Independently, the alumina powder was dispersed in propan-2-ol by an ultrasonic probe (IKA U200S, IKA Labortechnik Staufen, Germany) for 15 min. These were mixed to provide a ceramic/polymer mixture which has 60 vol% of ceramic powder based on the dry mass. After partial drying to reach a solvent level suitable for extrusion, the slurry became a paste with the final solvent content of 15 wt%. The pastes were extruded from a metal tube driven by a microextruder (micro-stepper motors (50,000 steps/

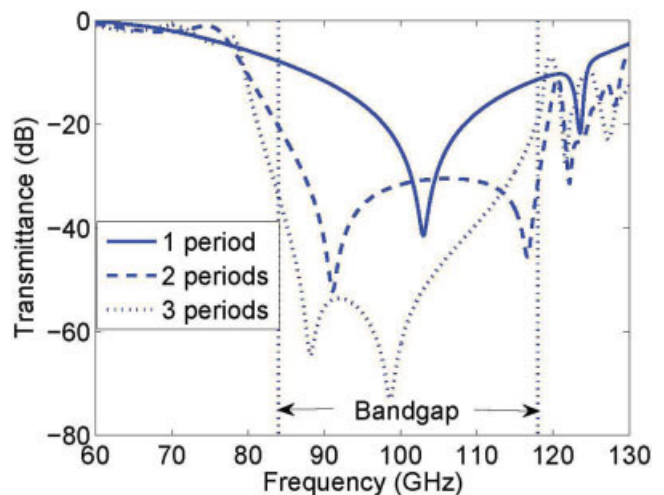


Figure 3 Simulated transmittance of woodpile EBG structure. [Color figure can be viewed in the online issue, which is available at www.interscience.wiley.com]

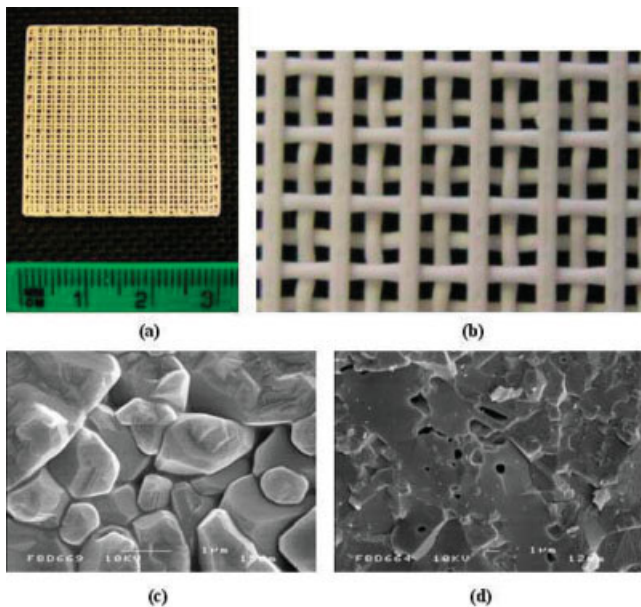


Figure 4 (a) Fabricated woodpile structure, (d) Details of the woodpile, SEM images of sample after sintering (c) from filament columnar section, (d) from filament surface direction. [Color figure can be viewed in the online issue, which is available at www.interscience.wiley.com]

rev) supplied by ACP & D, Ashton-under-Lyne, UK, with a 64–1 reduction box driving 1-mm-pitch ball screws (Automation, Oldham, UK) positioned over a three axis high performance linear motor table (MX80L Miniature Stage, Parker Hannifin Automation, Dorset, UK) capable of high acceleration (39.2 ms^{-2}) and speed (100 mms^{-1}) [6]. The extrusion dies of 400 and $500 \mu\text{m}$ by Quick-OHM (Sapphire waterjet cutting nozzle, model 1715) have been used. The table was driven by Labview software. After drying, the woodpile samples were heated at $2^\circ\text{C}/\text{min}$ to 400°C with a 1-h-dwell following $5^\circ\text{C}/\text{min}$ to 1540°C with another 1-h-dwell before furnace cooling to room temperature. The total linear shrinkage (dry shrinkage and sintering shrinkage) of the woodpile structure is 21%. Photos of the fabricated woodpile structure are shown in Figure 4.

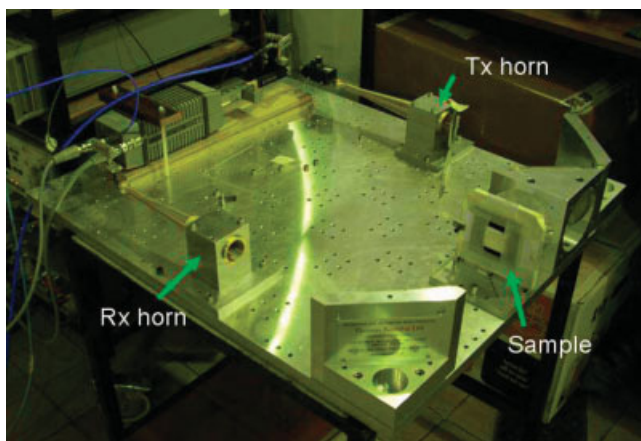


Figure 5 Photo of experimental setup for the measurement of transmission characteristics of woodpile EBG structures. [Color figure can be viewed in the online issue, which is available at www.interscience.wiley.com]

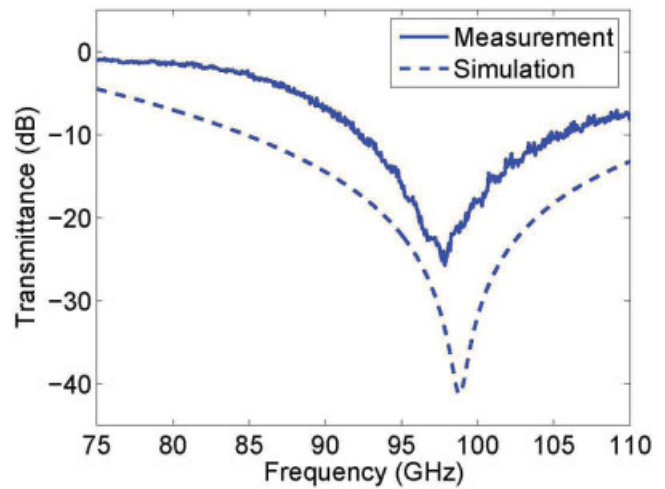


Figure 6 Comparison between the measured and simulated transmittances of the fabricated woodpile EBG structure. [Color figure can be viewed in the online issue, which is available at www.interscience.wiley.com]

4. MEASUREMENT RESULTS

We characterized the fabricated woodpile structures by performing transmission measurements using the millimeterwave transmitter and receiver. The millimeterwave source used for the measurement is capable of sweeping from 75 to 110 GHz. The fabricated woodpile structure was placed between the two identical circular horn antennas and a frequency sweep was performed to measure the transmission characteristic of the sample. To avoid diffraction from the edges of the sample, microwave absorbing materials were applied on the edges of the sample. The photo of the actual measurement setup is shown in Figure 5. We measured the woodpile samples in $30 \times 30 \text{ mm}^2$ size. The measured results are shown in Figure 6. The simulated results are also plotted for comparison. The simulated woodpile structure is assumed to be infinite. The actual physical parameters of the measured samples were $w = 0.41 \text{ mm}$, $a = 1.67 \text{ mm}$. The measured results show a good agreement with the simulated results, except slight offset in the transmittance level. The discrepancies in the transmittance level is attributed to the assumption (infinitely wide structure) made for the simulation showing higher attenuation along the direction of propagation.

5. CONCLUSIONS

In this letter, we have presented a woodpile EBG structure for millimeterwave applications fabricated by using a rapid prototyping technique based on extrusion freeforming. Numerical simulations have been performed for the design of millimeterwave woodpile structures. The fabricated woodpile structures have been measured. Experimental results showed a good agreement with the simulated results. The extrusion freeforming technique could be more flexible and versatile in realizing various microwave and millimeterwave structures.

ACKNOWLEDGMENT

The authors thank the Leverhulme Trust (F/07476/V) for the support of this research.

REFERENCES

1. E. Yablonovitch, Inhibited spontaneous emission in solid state physics and electronics, *Phys Rev Lett* 58 (1987), 2059.
2. J.D. Joannopoulos, R.D. Meade, and J.N. Winn, *Photonic crystals*:

Modeling the flow of light, Princeton University Press, Princeton, NJ, 1995.

3. Y.J. Lee, J. Yeo, K.D. Ko, R. Mittra, Y. Lee, and W. Park, A novel design technique for control of defect frequencies of an electromagnetic bandgap superstrate for dual-band directivity enhancement, *Microwave Opt Technol Lett* 42 (2004), 25–31.
4. A.R. Weily, L. Horvath, K.P. Essele, B. Sanders, and T. Bird, A planar resonator antenna based on woodpile EBG material, *IEEE Trans Antennas Propagat* 53 (2005), 216–223.
5. C.J. Reilly, W.J. Chappell, J.H. Halloran, and L.P.B. Katehi, High-frequency electromagnetic bandgap structures via indirect solid free-forming fabrication, *J Am Ceram Soc* 87 (2004), 1446–1453.
6. H. Yang, S. Yang, X. Chi, and J.R.G. Evans, Fine ceramic lattices prepared by extrusion freeforming, *J Biomed Mater Res B* 79 (2006), 116–121.
7. Y. Zhao and Y. Hao, Finite-difference time-domain study of guided modes in nano-plasmonic waveguides, submitted to *IEEE Trans Antennas Propagat*.
8. C.T. Chan and Q.L. Yu, Order-N spectral method for electromagnetic waves, *Phys Rev Lett* 51 (1995), 16635.
9. K.M. Ho, C.T. Chan, and C.M. Soukoulis, Existence of photonic gap in periodic dielectric structures, *Phys Rev Lett* 65 (1990), 3152.
10. X. Wang, X.G. Zhang, Q. Yu, and B.N. Harmon, Multiple scattering theory for electromagnetic waves, *Phys Rev Lett B* 47 (1993), 4161.
11. M.N. Afsar and K.J. Button, Millimeter-wave dielectric measurement of materials, *Proc IEEE* 73 (1985), 131–153.

© 2007 Wiley Periodicals, Inc.

GEOMETRICALLY BASED POWER AZIMUTH SPECTRUM MODELS FOR MOBILE COMMUNICATION SYSTEMS

Lei Jiang¹ and Soon Yim Tan²

¹ Fraunhofer Institute for Telecommunications, Heinrich-Hertz-Institut, Einsteinufer 37, D-10587 Berlin, Germany

² School of EEE, Nanyang Technological University, 50 Nanyang Avenue, Singapore 639798

Received 2 February 2007

ABSTRACT: A geometrically based single bounce power azimuth spectrum model for mobile communication systems is proposed in this article. The scatterers are assumed to distribute around the transmitting antenna within a circular region. The distribution of the scatterers can be arbitrary, e.g., Rayleigh, exponential etc. Power azimuth spectrums are derived for these propagation environments. Comparisons between our theoretical calculations and the empirical results as well as the measurement data reported in the literature show that the Rayleigh distribution scatterer models is applicable for the outdoor microcell propagation environment, while the exponential distribution scatterer model is accurate for the indoor office/laboratory propagation environment. © 2007 Wiley Periodicals, Inc. *Microwave Opt Technol Lett* 49: 2093–2097, 2007; Published online in Wiley InterScience (www.interscience.wiley.com). DOI 10.1002/mop.22686

Key words: power azimuth spectrum; Rayleigh; exponential

1. INTRODUCTION

With the advent of smart antenna systems for both interference cancellation and position location applications, in addition to signal power level, the spatial and temporal properties of the channel have an enormous impact on the performance of the system. Hence the propagation channel models providing the information about the spatial and temporal properties are needed. Geometrically based single bounce models [1–8] have been shown to be an

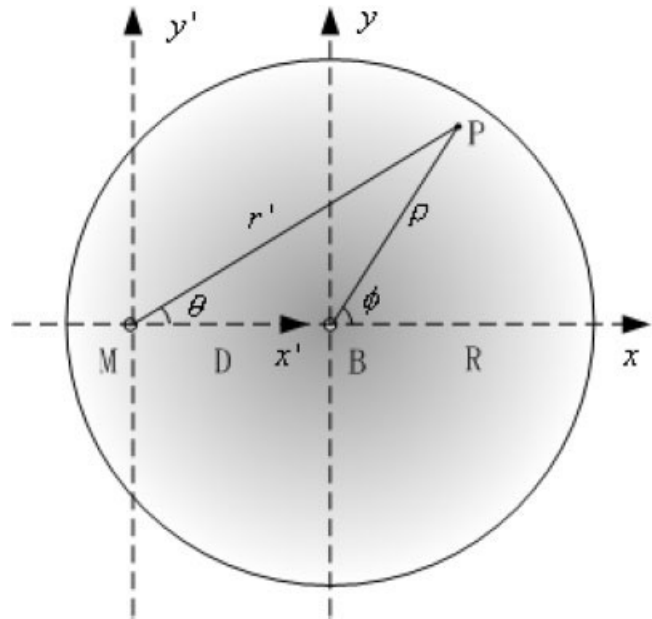


Figure 1 Scatterer geometry

effective way to investigate these statistical characteristics. Liberti and Rappaport [1] developed a statistical model for microcell communication system assuming that the scatterers are uniformly distributed inside an ellipse with foci at the base station and the mobile receiver. The circular scattering macrocell channel model [2] assumes that the scatterers are uniformly distributed within a circle around the mobile receiver, and the base station is outside this area [3] proposed a more general approach that the probability density functions (pdf) for both elliptical [1] and circular [2] scattering models can be derived using a common approach [4] described an analytical channel model based on the assumption that omnidirectional scatterers are distributed uniformly on a two-dimensional hollow-disc centered upon the mobile. By varying the hollow disc's thickness, this spatial density degenerates to the well-know uniform-ring or uniform-disc density [2, 3]. However, all these models focus on the pdfs of the angle of arrival (AOA) and time of arrival (TOA), no power spectrum has been analyzed. In our previous papers [9, 10], a geometrically based single bounce model was proposed, which assumes that the scatterers are uniformly distributed around the base station within a circular region of radius R , where R can be determined by the coverage area of the base station. In [11], the uniform distribution scatterer model is extended to a more general case, where the scatterers can be of any distribution. Rayleigh distribution and exponential distribution are used to model the outdoor microcellular and indoor office/laboratory propagation environment. In this article, the power azimuth spectrum (PAS) for these models will be investigated.

The article is organized as follows. In Section 2, a general formulation of the model is given, and the derivation of the power azimuth spectrum is outlined. The PASs for the Rayleigh distribution scatterer model and the exponential distribution scatterer model are analyzed in Section 3. Section 4 is the conclusion of our work.

2. THEORY AND FORMULATION

2.1. The Geometrically Based Channel Models

Figure 1 shows the geometry of the scatterers around the base station B . The mobile receiver is marked as M (without loss of